Journal of Materials Chemistry

Cite this: J. Mater. Chem., 2012, 22, 17236

www.rsc.org/materials

PAPER

Novel solution-processable optically isotropic colorless polyimidothioethers–TiO_2 hybrids with tunable refractive index†

Chia-Liang Tsai,[a] Hung-Ju Yen,[a] Wen-Chang Chen[ab] and Guey-Sheng Liou*[a]

Received 20th April 2012, Accepted 21st June 2012
DOI: 10.1039/c2jm32480f

In this study, a new facile synthetic route was developed to prepare polyimidothioethers–nanocrystalline-titania (PITEs–TiO_2) hybrid optical films with a high titania content (up to 50 wt%) and thickness (15 ± 3 μm) from soluble PITEs containing hydroxyl groups. A series of organosoluble PITEs were prepared from the hydroxy-substituted dithiols and various commercial bismaleimides *via* Michael polyaddition. The hydroxyl groups at the backbone of the PITEs could provide the organic–inorganic bonding sites and resulted in homogeneous hybrid solutions by controlling the mole ratio of titanium butoxide/hydroxyl group. AFM, TEM, and XRD results indicated the formation of well-dispersed nanocrystalline-titania. The flexible hybrid films were successfully obtained and revealed good surface planarity, thermal dimensional stability, tunable refractive index (1.69 to 1.80 at 633 nm), and high optical transparency. A three-layer antireflection coating based on the hybrid films was prepared and showed a reflectance of less than 0.5% in the visible range, indicating its potential optical applications.

Introduction

High refractive index polymers have been widely proposed in recent years for their potential in advanced optoelectronic applications.[1–4] In addition to the basic parameter of the refractive index, others such as birefringence, Abbe's number, optical transparency, processability, and thermal stability are often taken into consideration. Regarding the encapsulation for organic light-emitting diodes (OLEDs),[2] commercial applications require materials with a high refractive index, low birefringence, high optical transparency, and a long-term ultraviolet light and thermal stability. Therefore, achieving a good combination of the above-mentioned parameters is a crucial and ongoing issue.[5–7] Recently, systematic work by Ueda revealed the influence of sulfur groups and related structures on the refractive index and optical dispersion of the resulted polyimides.[7] The incorporation of sulfur atom into polymer systems could enhance the refractive index and optical transparency due to its large atomic refraction.[8–10] Recently, we also reported that the materials derived from bismaleimides (BMIs) *via* Michael polyaddition could exhibit not only excellent optical characteristics, but also high thermal stability and mechanical properties, thus making them an available thermoplastic encapsulation candidate for organic light-emitting diodes (OLEDs).[11]

Polymer–inorganic hybrid materials have recently attracted considerable interest owing to their enhanced mechanical, thermal, magnetic, optical, electronic, and optoelectronic properties when compared to the corresponding individual polymer or inorganic component.[12–14] Chemical methods based on an *in situ* sol–gel hybridization approach made it possible to manipulate the organic–inorganic interfacial interactions at various molecular and nanometer length scales, resulting in homogeneous structures and thus overcoming the problem of nanoparticle agglomeration.[15] The obtained polyimide–titania (PI–TiO_2) hybrid materials also could be further processed by hydrothermal treatment to induce the nanocrystalline titania domain.[16]

In the present study, we describe a facile synthesis of optically transparent and thermoplastic polyimidothioethers (PITEs) having hydroxyl groups and their titania hybrid films. The lateral hydroxyl groups in the PITE backbone could provide the organic bonding sites with inorganic titania, thus highly homogeneous hybrid films with different TiO_2 contents could be successfully obtained.

Experimental section

Materials

4,4′-(Diaminodiphenylsulfide)bismaleimide (S-BMI)[17] (mp: 187 °C) and 4,4′-(diaminodiphenylsulfone)bismaleimide (SO_2-BMI)[18] (mp: 252 °C) were readily synthesized by reacting the

[a]*Institute of Polymer Science and Engineering, National Taiwan University, 1 Roosevelt Road, 4th Section, Taipei 10617, Taiwan. E-mail: gsliou@ntu.edu.tw*
[b]*Department of Chemical Engineering, National Taiwan University, 1 Roosevelt Road, 4th Section, Taipei 10617, Taiwan*
† Electronic supplementary information (ESI) available. See DOI: 10.1039/c2jm32480f

respective diamines with maleic anhydride according to the reported procedure. Commercially available monomers such as 4,4′-(diaminodiphenylmethane)bismaleimide (CH_2-BMI), (2*S*,3*S*)-1,4-disulfanylbutane-2,3-diol (DT-OH), and 4,4′-thiobisbenzenethiol (DT-S) were used as received. All other reagents were used as received from commercial sources.

Polymer synthesis

According to the Michael polyaddition technique described by Crivello,[19] a series of new PITEs with high refractive index and optical transparency were synthesized from the readily obtainable BMIs and dithiols (Scheme 1). The polymerization proceeded homogeneously throughout the procedure, affording clear and viscous polymer solutions in high yields with no evolution of volatile molecules. All the polymers precipitated in a white fiber-like form when slowly pouring the resulting polymer solutions into acidified methanol. The obtained PITEs had inherent viscosities in the range of 0.33–1.25 dL g^{-1} (measured at a concentration of 0.5 g dL^{-1} in DMAc at 30 °C). Infrared spectroscopy (FT-IR) was used to identify the structures of the PITEs. For **S-OHS**, 3000–3750 cm^{-1} (O–H stretch), 1781 cm^{-1} (asym. C=O str.), 1713 cm^{-1} (sym. C=O str.), 1383 cm^{-1} (C–N), 1082 cm^{-1} (Ar–S–Ar str.), 748 cm^{-1} (imide ring deformation), respectively; ^{1}H NMR (DMSO-d_6, δ, ppm): 2.69–3.43 (m,12H), 3.55 (OH), 4.13–4.22 (m, 2H), 4.55 (m,2H), 5.20 (m,2H), 7.17(d, 2H), 7.29 (d, 2H), 7.44 (d, 2H), 7.51 (d, 2H). Anal. calcd (%) For **S-OHS** $(C_{58}H_{50}N_4O_{10}S_7)_n$ $(1187.49)_n$: C, 58.66; H, 4.24; N, 4.72; S, 18.90. Found: C, 56.65; H, 3.97; N, 4.69; S, 18.62. The other PITEs were prepared from the corresponding bismaleimide and dithiol by a similar procedure to the one described above.

Preparation of the PITE films

N,*N*-Dimethylacetamide (DMAc) solutions of the PITEs were drop-coated onto fused silica (amorphous SiO_2) or glass substrates and dried at 80 °C for 6 h, and then 150 °C for 8 h under vacuum condition. PITE films with thicknesses around 20 μm could be prepared and used for solubility tests, refractive index, transmittance, and thermal analyses.

Preparation of the PITE–titania hybrid films

The preparation of PITE–titania hybrid **S-OHS50** was used as an example to illustrate the general synthesis route used to produce the hybrid **S-OHSX** (Scheme 2). Firstly, 0.12 g (0.18 mmole) of **S-OHS** was dissolved in 6.0 mL of DMAc, and then 0.20 mL of HCl (37 wt%) was added very slowly into the PITE solution and further stirred at room temperature for 30 min. Then, 0.50 mL (1.46 mmole) of $Ti(OBu)_4$ dissolved in 0.50 mL of butanol was added drop-wise into the above solution by a syringe, and then stirred at room temperature for 30 min. Finally, the resulting precursor solution of **S-OHS50** was filtered through a 0.45 mm PTFE filter and poured into a 6 cm glass Petri dish. The hybrid optical thick film could be obtained by a subsequent heating program at 60 °C for 6 h, 110 °C for 3 h under vacuum conditions. In addition, the above prepared solution was also spin-coated onto a glass plate or silicon wafer at 1000–3000 rpm for 30 s. The obtained film was then treated by the multi-step heating process of 60 °C and 80 °C for 30 min, and 110 °C for 60 min, respectively, to afford the hybrid thin film. Then, these resulting PITE–titania hybrid thick and thin film were further treated *via* a hydrothermal process by immersing them into the water vapor at 100 °C for 12 h. After the above process, the films were dried at 100 °C and the hybrid thick films and thin films could be obtained with thicknesses of 15–20 μm and 253–325 nm, respectively. Thus, a series of flexible, transparent, and well nano-scale dispersed PITE–TiO_2 hybrid optical films with different titania contents could be successfully prepared.

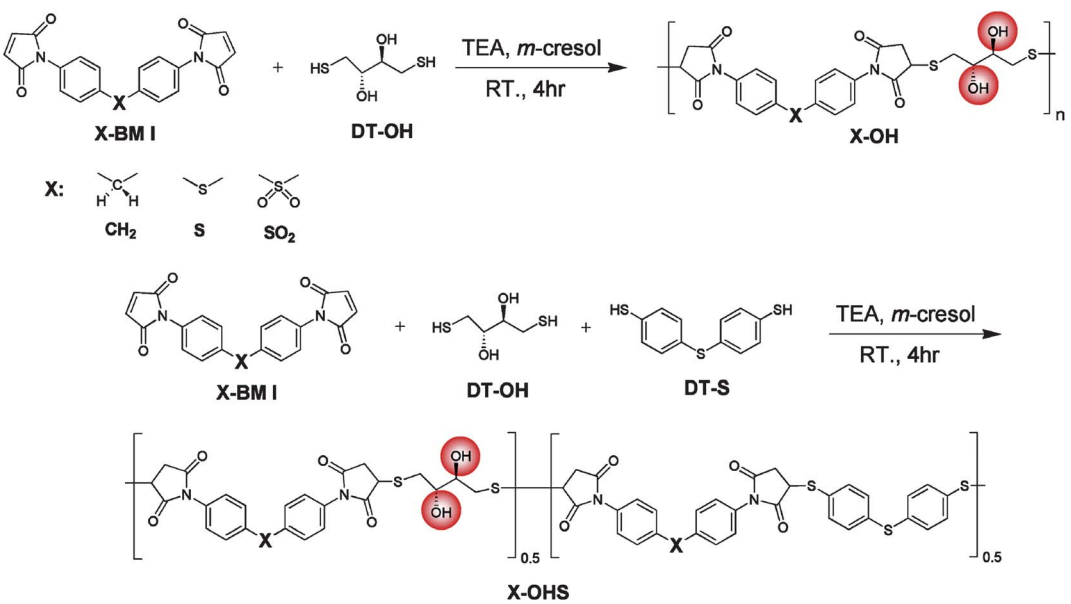

Scheme 1 Michael polyaddition of polyimidothioethers.

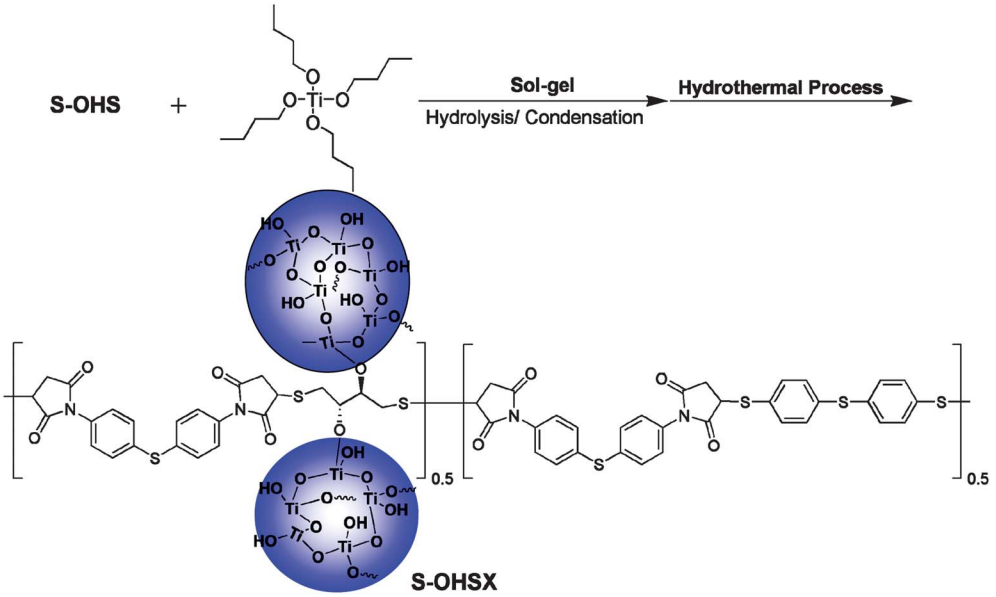

Scheme 2 Preparation of polyimidothioethers (PITEs)–nanocrystalline-titania hybrids.

Table 1 Inherent viscosities and GPC data of polyimidothioethers

Index	η_{inh}[a]/dL g^{-1}	M_w[b]	M_n[b]	PDI[c]
CH_2-OH	1.25	133700	59400	2.25
S-OH	1.01	132100	60500	2.18
SO_2-OH	0.35	103700	53100	1.95
CH_2-OHS	0.46	123700	51100	2.42
S-OHS	0.50	120500	57600	2.09
SO_2-OHS	0.33	119700	66100	1.81

[a] Measured at a polymer concentration of 0.5 g dL^{-1} in DMAc at 30 °C. [b] Calibrated with polystyrene standards, using NMP as the eluent at a constant flow rate of 0.5 mL min^{-1} at 40 °C. [c] Polydispersity index (M_w/M_n).

Measurements

Fourier transform infrared (FT-IR) spectra were recorded on a PerkinElmer Spectrum 100 Model FT-IR spectrometer. Elemental analyses were run in a Heraeus VarioEL-III CHNS elemental analyzer. ^{1}H spectra were measured on a JEOL JNM-AL 300 MHz spectrometer in DMSO-d_6, using tetramethylsilane as an internal reference. The inherent viscosities were determined at 0.5 g dL^{-1} concentration using Tamson TV-2000 viscometer at 30 °C. Thermogravimetric analysis (TGA) was conducted with a PerkinElmer Pyris 1 TGA. Experiments were carried out on approximately 6–8 mg film samples heated in flowing nitrogen or air (flow rate = 20 cm^3 min^{-1}) at a heating rate of 20 °C min^{-1}. Coefficients of thermal expansion (CTE) and softening temperatures (T_s) were measured by thermomechanical analysis (TMA) with a TMA Q400, TA Instruments. The experiments were conducted from 50 °C to 300 °C at a scan rate of 10 °C min^{-1} with a penetration probe 1.0 mm in diameter under an applied constant load of 10 mN. The softening temperature (T_s) was taken as the onset temperature of probe displacement on the TMA traces, and the CTE data were determined in the range 50–150 °C by expansion mode. Ultraviolet-visible (UV-vis) spectra of the polymer films were recorded on Hitachi U-4100 UV-vis-NIR spectrophotometer. An ellipsometer (SOPRA, GES-5E) was used to measure the refractive index (n) of the prepared films in the wavelength range of 300–800 nm. The thickness (n) of the prepared film was also determined simultaneously. In-plane (n_{TE}), and out-of plane (n_{TM}) refractive indices of the films formed on the silica substrates were measured using a prism coupler (Metricon, PC-2000) at wavelengths of 632.8 nm at room temperature. The mean refractive indices (n_{av}) were calculated as $n_{av}^2 = (2n_{TE}^2 + n_{TM}^2)/3$. The in-plane/out-of-plane birefringence (Δn) was calculated as $\Delta n = n_{TE} - n_{TM}$.

Results and discussion

Synthesis of PITEs and hybrid materials

According to the Michael polyaddition technique described by Crivello,[19] a novel series of PITEs with high molecular weights, high refractive index, and optical transparency were synthesized from the readily obtained BMIs and dithiols at room temperature for 4 h in the presence of a catalytic amount of triethylamine as a basic catalyst in *m*-cresol (Scheme 1). The polymerization proceeded homogeneously throughout the procedure and afforded clear, viscous polymer solutions in high yields with no evolution of volatile molecules. All the polymers precipitated in a white fiber-like form when slowly pouring the resulting polymer solutions into acidified methanol. The inherent viscosities (η_{inh}) in the range of 0.33–1.25 dL g^{-1}, the weight average molecular weights (M_w), and the polydispersity index (PDI) of the obtained PITEs are listed in Table 1. Furthermore, the structural composition of PITEs was confirmed by the NMR spectra in DMSO-d_6 shown in Fig. 1, where the spectrum of copolymer **S-OHS** demonstrated very well with the combination of corresponding individual molecular structure of **S-S** and **S-OH**.

The PITEs were readily soluble in polar aprotic organic solvents such as NMP, DMAc, *N*,*N*-dimethylformamide (DMF), and dimethyl sulfoxide (DMSO), and the results are

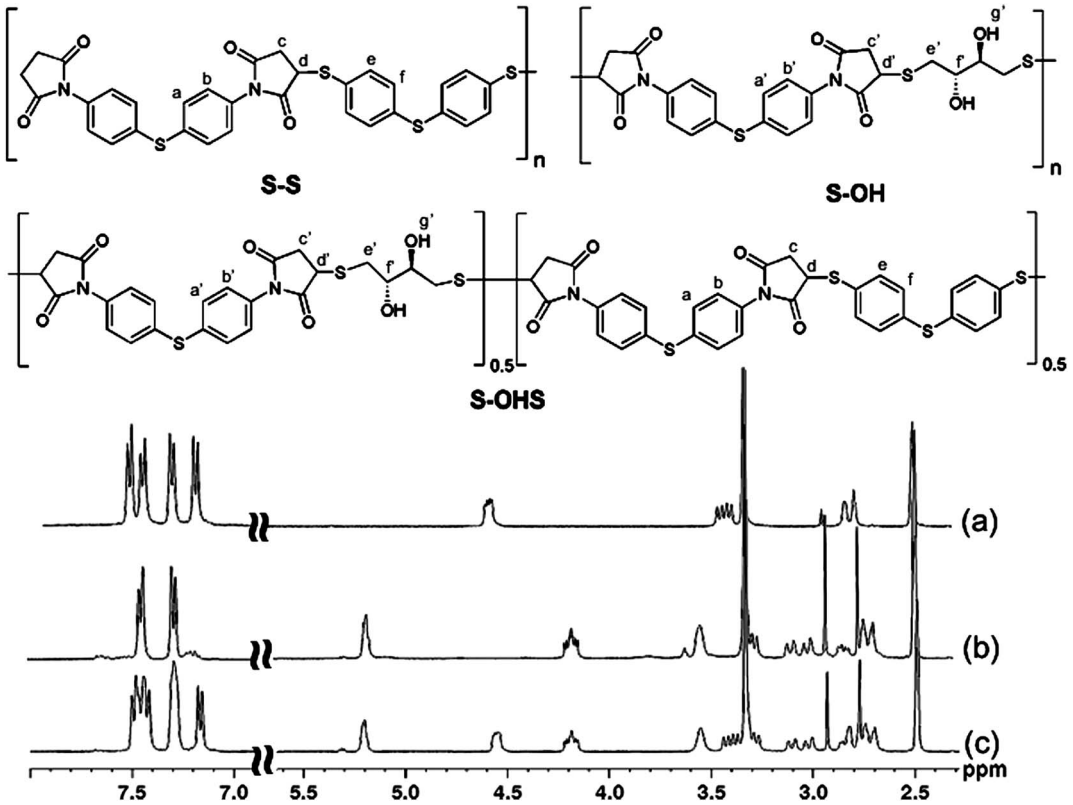

Fig. 1 ^{1}H NMR spectra of PITE (a) **S-S** (b) **S-OH**, and (c) **S-OHS** in DMSO-d_6.

summarized in Table 2. Furthermore, the PITEs could be solvent cast into flexible, transparent, and tough films (Fig. 2). Therefore, these novel high performance thin films could be prepared by spin-coating or inkjet-printing processes for practical optical applications.

The fabrication procedure for hybrid films from PITEs and titania precursors is depicted in Scheme 2, and the reaction compositions are also summarized in Table 3. The flexible, transparent, and homogeneous PITE–nanocrystalline-titania (**S-OHSX**) hybrid optical films with different titania contents could be successfully prepared, and the appearance of **S-OHS10** and **S-OHS30** thick optical hybrid films is also displayed in Fig. 3. The FTIR spectra (Fig. S1†) of the **S-OHS** and **S-OHS50** films show a broad absorption band in the region 3000–3750 cm^{-1} (O–H stretch) and characteristic imide absorption bands at 1781 cm^{-1} (asym. C=O str.), 1713 cm^{-1} (sym. C=O str.), 1383 cm^{-1} (C–N), 748 cm^{-1} (imide ring deformation), and 1082 cm^{-1} (Ar–S–Ar str.), respectively. The absorption peak of the polyimide–titania thin film, **S-OHS50**, at 3000–3750 cm^{-1} might be attributed to the hydroxyl groups of the titania crystalline. In addition, the inorganic Ti–O–Ti band could also be observed at 650–800 cm^{-1}, which is also similar to that in the previous report.[20]

Thermal properties of PITE and hybrid films

The thermal properties of PITEs were examined by TGA (Fig. S2†) and TMA, and the results are summarized in Table 4. All the prepared PITEs exhibited good thermal stability with insignificant weight loss up to 270 °C under a nitrogen

Table 2 Solubility behavior of polyimidothioethers

	Solubility in various solvents[a]						
Polymer	NMP	DMAc	DMF	DMSO	*m*-Cresol	THF	$CHCl_3$
CH_2-OH	++	++	++	+–	++	–	–
S-OH	++	++	++	+–	++	–	–
SO_2-OH	++	++	++	+–	++	–	–
CH_2-OHS	++	++	++	+–	++	–	–
S-OHS	++	++	++	+–	++	–	–
SO_2-OHS	++	++	++	+–	++	–	–

[a] The solubility was determined with a 50 mg sample in 1 mL of a solvent. ++, soluble at room temperature; +–, partially soluble; –, insoluble even on heating.

Fig. 2 Representative flexible and highly transparent PITE and Kapton films (thickness ~20 μm).

atmosphere. The softening temperature (T_s) of PITEs observed in the range 80–110 °C could be easily measured by the TMA thermograms. Thus, the melting-process window (ΔT) termed as the region between the softening temperature (T_s) and the initial decomposition temperature (T_d) for these materials were in the range 170–220 °C, exhibiting great potential feasibility for injection molding processes. Furthermore, the thermal behavior of the polyimide–nanocrystalline-titania hybrids was evaluated by TGA, TMA and DMA, and the results are listed in Table 5. The TGA curves (Fig. S3 and S4†) of all these hybrid materials both in nitrogen and air revealed excellent thermal stability and increased carbonized residue (char yield) with increasing titania content. The titania contents in the hybrid materials could be estimated based on the char yields under air flow, which were in good agreement with the theoretical content and ensured successful incorporation of the nanocrystalline-titania. On the other hand, the initial weight loss could not be found before 300 °C for these PITE–titania hybrid materials, which provided more evidence of completely organic–inorganic bonding. The typical TMA thermogram (Fig. S5 and S6†) for **S-OHS** and the corresponding hybrid materials revealed that the softening temperature increased from 103 °C to 231 °C with increasing titania content. In addition, the thermal behavior such as glass transition temperature (T_g), storage modulus (E'), and tan δ of the polymer and hybrid films were also evaluated by DMA and depicted in Fig. 4. The T_g and E' could be enhanced gradually with increasing titania content, which restricted the segmental chain mobility by crosslinking between PITE chains and titania clusters. Meanwhile, CTE is one of the important designing parameters for the application of polymer films in the micro-electronic field, the CTE of the pure PITE film and the PITE–nanocrystalline-titania hybrid films were measured and are summarized in Table 4. Generally, inorganic reinforced components often revealed much lower CTE values than that of organic matrices, which suppressed CTE of the resulting hybrid materials. Therefore, CTE of the organic–inorganic hybrids decreased with increasing the volume fraction of inorganic reinforcement.

Fig. 3 Representative flexible and highly transparent PITE hybrid films (thickness: 15 ± 3 μm).

Table 4 Thermal and optical properties of polyimidothioethers

	Thermal properties/°C			Optical properties		
Index	T_s[a]	T_d[b]	ΔT[c]	λ_0/nm[d]	n[e]	Δn[f]
CH_2-OH	80	300	220	310	1.637	0.0031
S-OH	85	305	220	327	1.660	0.0018
SO_2-OH	92	270	178	312	1.648	0.0045
CH_2-OHS	85	305	220	336	1.672	0.0005
S-OHS	103	315	212	338	1.692	0.0010
SO_2-OHS	110	280	170	337	1.680	0.0022
Kapton				452	1.687	0.0770

[a] Softening temperature measured by TMA with a constant applied load of 10 mN at a heating rate of 10 °C min^{-1} by penetration mode. [b] Initial decomposition temperature recorded by TGA. [c] The melting-process window (ΔT) was calculated as $\Delta T = T_d - T_s$. [d] The cutoff wavelength (λ_0) from the UV-vis transmission spectra of polymer films (thickness ~20 μm). [e] Refractive index at 633 nm by ellipsometer. [f] The in-plane/out-of-plane birefringence (Δn) was calculated as $\Delta n = n_{TE} - n_{TM}$ were measured using a prism coupler.

Optical properties of PITE and hybrid films

The UV-visible (UV-vis) absorption spectra of PITE films (thickness: 20 μm) are presented in Fig. 5. All the polymer films

Table 3 Reaction composition and properties of the **S-OHS** hybrid films

	Reactant composition/wt%		Hybrid film TiO_2 content/wt%				
Polymer	**S-OHS**	$Ti(OBu)_4$	Theoretical	Experimental[a]	h[b]/nm	R_q[c]/nm	n[d]
S-OHS	100	0	0	0	253	2.035	1.69
S-OHS10	67.8	32.2	10	9.8	271	1.874	1.72
S-OHS30	35.4	64.6	30	28.3	284	1.263	1.77
S-OHS50	19.0	81.0	50	49.4	325	0.951	1.80

[a] Experimental titania content estimated from TGA curves. [b] h: film thickness. [c] R_q: the root mean square roughness. [d] n: refractive index at 633 nm by ellipsometer.

Table 5 Thermal properties of **S-OHS** hybrid film

Polymer	T_g[a]	T_s[b]	CTE/ppm K^{-1}[c]	T_d^5/°C[d] N_2	T_d^5/°C[d] Air	T_d^{10}/°C[d] N_2	T_d^{10}/°C[d] Air	R_{w800}/%[e]
S-OHS	129	103	88	320	325	345	355	33
S-OHS10	191	172	72	380	405	450	470	61
S-OHS30	231	205	57	400	410	460	470	69
S-OHS50	248	231	45	415	420	470	475	76

[a] Glass transition temperature was performed by DMA on PI film specimens (15 mm long, 8 mm wide, and 20–30 mm thick) at a heating rate of 3 °C min^{-1} with a load frequency of 1 Hz in air. [b] Softening temperature measured by TMA with a constant applied load of 10 mN at a heating rate of 10 °C min^{-1} by penetration mode. [c] The CTE data was determined over a 50–150 °C range by expansion mode. [d] Temperature at which 5% and 10% weight loss occurred, respectively, recorded by TGA at a heating rate of 20 °C min^{-1} and a gas flow rate of 30 cm^3 min^{-1}. [e] Residual weight percentages at 800 °C under nitrogen flow.

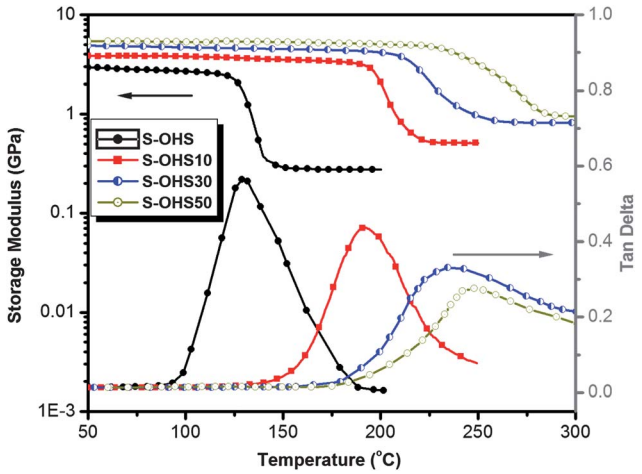

Fig. 4 Storage modulus and tan delta curves of **S-OHS** hybrid materials.

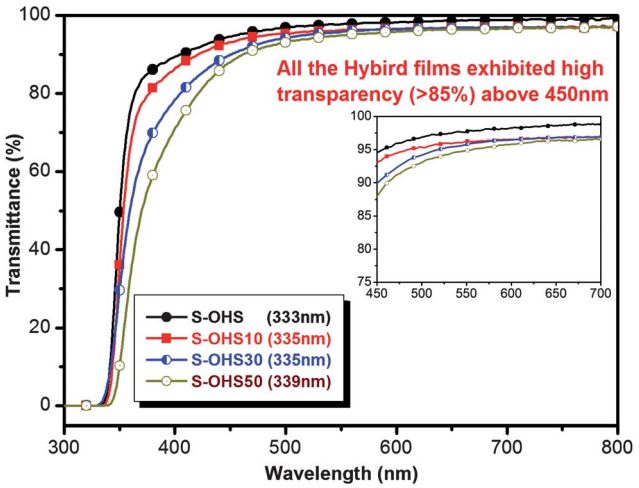

Fig. 6 Transmittance UV-visible spectra of **S-OHS** hybrid thick films (thickness: 15 ± 3 μm).

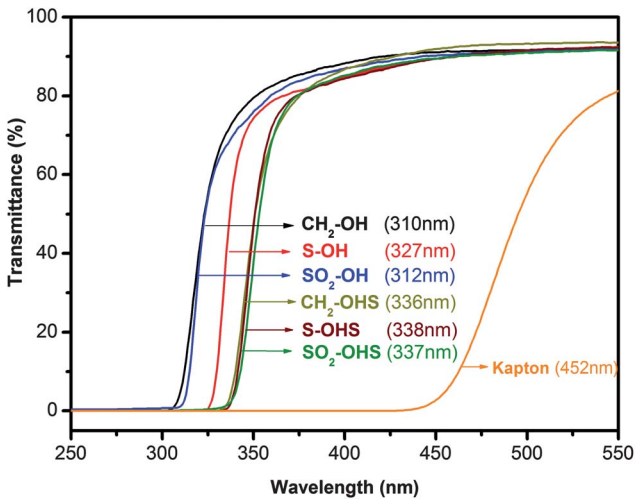

Fig. 5 Transmittance UV-visible spectra of **PITEs** thick films (thickness: ~20 μm).

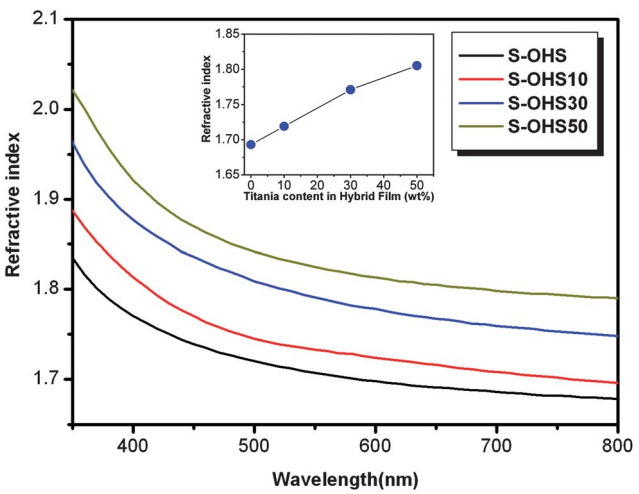

Fig. 7 Variation of the refractive index of the **S-OHS** hybrid materials with wavelength. The inset figure shows the variation of refractive index at 633 nm with titania content.

exhibited high transparency (>85%) in the visible region (wavelengths: 400–800 nm). The coefficients of n and Δn are listed in Table 2. The values of n and Δn having potential for optical applications are 1.692 and 0.0010 for PITE **S-OHS**, respectively, whereas the (n, Δn) values for Kapton is (1.687, 0.0770). To the best of our knowledge, these new PITEs exhibit a notable result of optically isotropic characteristic with the ultra-lowest birefringence value of 0.0005, compared with other high refractive index

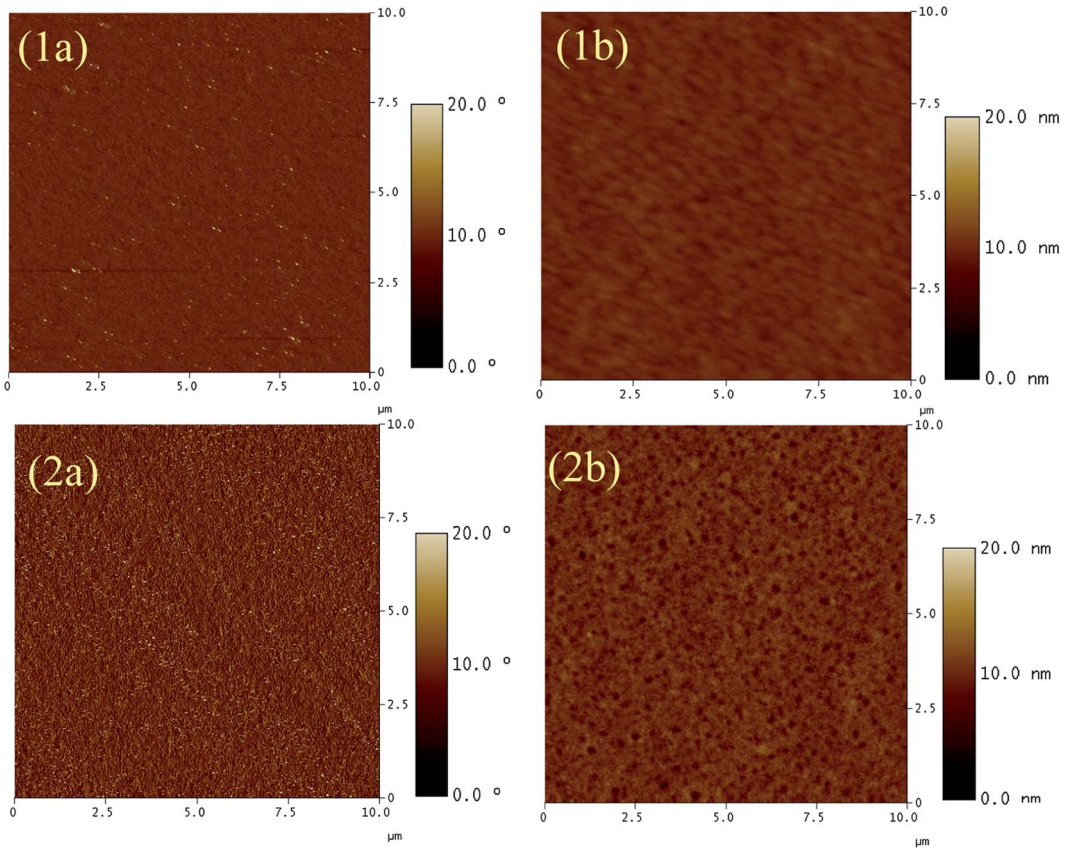

Fig. 8 AFM images of the **S-OHS30** hybrid films coated on glass: (1a) phase images (1b) height images; **S-OHS50** hybrid films coated on glass: (2a) phase images (2b) height images.

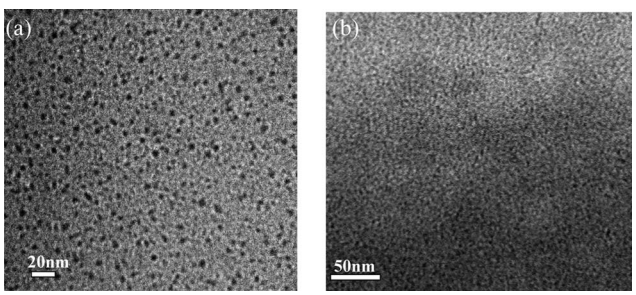

Fig. 9 TEM image of the hybrid material **S-OHS50**: (a) top view (b) cross-section.

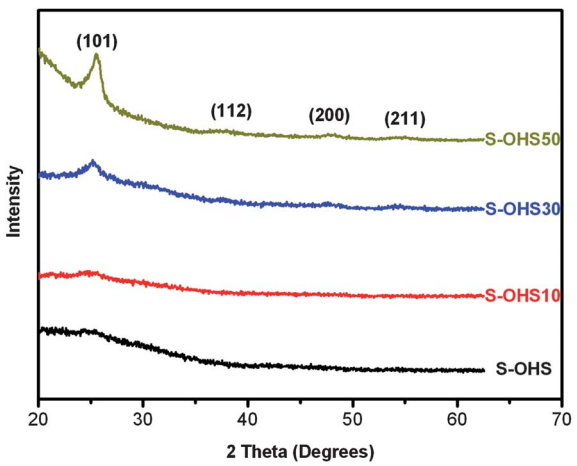

Fig. 10 XRD patterns of the **S-OHS** and **S-OHS10**–**S-OHS50** hybrid materials.

polyimides.[5] Furthermore, the UV-vis spectra of the **S-OHS** hybrid thick films were also investigated for comparison, and the results are summarized in Fig. 6. These thick hybrid films also revealed much higher optical transparency and lower cutoff wavelengths in the UV region than that of the Kapton film, indicating that highly homogeneous dispersed PITE–nano-crystalline titania hybrid materials have been obtained. The cutoff wavelength increased and the corresponding band edge also red-shifted with increasing titania content, such a phenomena could usually be observed for titania sizes less than 10 nm.[20]

The refractive index dispersion of the obtained **S-OHS** hybrid films at wavelengths of 350–800 nm is depicted in Fig. 7, and the inset figure shows the variation of refractive index at 633 nm with titania content. The refractive index increased linearly with increasing titania contents, implying that the Ti–OH groups of the hydrolyzed precursors condensed progressively to form the Ti–O–Ti domain structures, which resulted in an enhanced refractive index. These results also demonstrate that using a soluble PITE with hydroxyl groups at each repeating unit is a facile and successful approach for preparing titania hybrid materials. Furthermore, the refractive index of the hybrid films can be enhanced, obviously owing to the TiO_2 in the hybrid film,

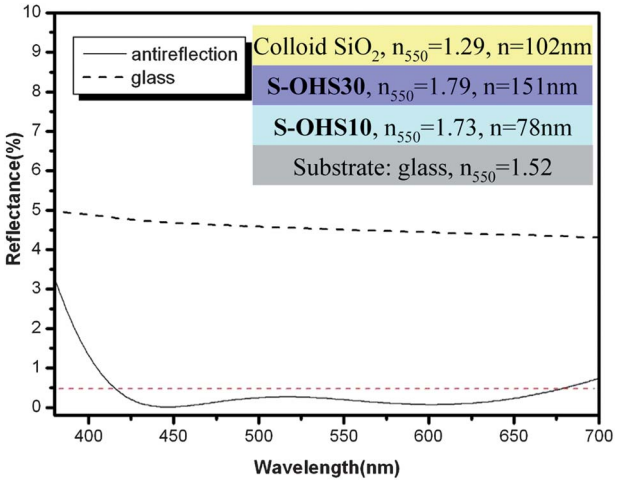

Fig. 11 Variation of the reflectance with wavelength: slides and the three-layer antireflection coating.

which can be crystallized *via* hydrothermal treatment. Combining the issues of thickness, flexibility, and optical transparency, the PITE–titania hybrid optical thick film **S-OHS50** (15 ± 3 μm in thickness) showed the best optical transparency with a high refractive index, up to 1.80 at 633 nm.

Morphology analyses

The height and phase AFM images of **S-OHS30** and **S-OHS50** thin films were summarized in Fig. 8. The results of root mean square surface roughness (R_q) for the hybrid films analyzed by AFM were listed in Table 3. The ratio of surface roughness to film thickness (R_q/h) was less than 0.15% implying the excellent surface planarity of the hybrid films could be obtained. These results demonstrated that the hydroxyl groups attached on the PITE backbone played an important role for providing the bonding sites with titania and effectively improving the dispersion and morphological stability of the inorganic titania in the hybrid materials. Furthermore, the TEM images of the **S-OHS50** film are shown in Fig. 9a (top view) and Fig. 9b (cross-section), and exhibit the titania nanocrystallites well-dispersed in the hybrid material with the average domain size in the range of 3–5 nm. The XRD patterns of the hybrid films depicted in Fig. 10 revealed that the matrix PITE hybrid materials was amorphous and the intensity of a titania crystalline peak gradually increased in the range 2θ = 23–27° with increasing titania content suggesting that the titania clusters were well dispersed in PITEs due to the hydrolysis–condensation reactions occurring between $Ti(OBu)_4$ and pendant hydroxyl groups of PITEs. The enhanced titania crystallization could be obviously observed in **S-OHS50** with four peaks, 25.5°, 38.4°, 48.3°, and 54.8°, corresponding to the (101), (112), (200), and (211) crystalline planes of the anatase titania phase, respectively.[21–23] The broad width of the peaks were due to the scattering of X-rays, resulting from the small size of the titania nanocrystalline grains.

Multilayer antireflection coatings

The structure of the three layer anti-reflective coating on the glass substrate and the reflectance spectra are depicted in Fig. 11. The glass substrate exhibited a refractive index (n = 1.52) higher than air (n = 1.0) and revealed an average reflectance of about 4.5% in the visible range. The reflectance could be reduced significantly *via* the three-layer antireflection coating consisting of colloid SiO_2, **S-OHS30**, and **S-OHS10** for the first, second, and third layer, respectively. In order to reduce reflection through adjusting the phase of light, the optical thickness (physical thickness × refractive index) was designed to be 0.25 λ_0, 0.5 λ_0, and 0.25 λ_0 (λ_0 = 550 nm) for the three-layer structure. Thus, the thickness and refractive index of the resulting films of colloid SiO_2, **S-OHS30**, and **S-OHS10** were 102 nm (1.29), 151 nm (1.79), and 78 nm (1.73), respectively. As shown in Fig. 11, the reflectance of the prepared anti-reflection coatings was less than 0.5% in the visible range (400 nm to 700 nm), which was significantly smaller than that of the glass with 4.5%. It suggested the potential application of the prepared polyimide–titania hybrid films in optical devices.

Conclusion

By this facile approach, a series of thermoplastic PITEs could be readily prepared from the respective BMIs and dithiols *via* a Michael polyaddition. The obtained polymers showed an useful thermal processing window up to 190 °C. All the amorphous polymers exhibited high optical transparency with a cutoff wavelength in the range of 312–338 nm and a high refractive index in the range of 1.63–1.69. Moreover, the relatively low birefringence of 0.0005 could also be achieved. In addition, this PTIE containing hydroxyl group could provide the organic–inorganic bonding with titanium butoxide ($Ti(OBu)_4$) by sol–gel and highly homogeneous hybrid films could be obtained. A three-layer antireflective coating based on the hybrid films exhibited a reflectance of less than 0.5% in the visible range (400–700 nm). Furthermore, the thick titania hybrid films could be achieved even with the relatively high titania content (50 wt%) and refractive index (1.80), implying potential optical applications of these novel polyimide–titania hybrid optical films.

Acknowledgements

The authors are grateful to the National Science Council of Taiwan for financial support of this work, and also to Dr Shing-Jong Huang of the Instrumentation Center, National Taiwan University, for help in measuring solid-state NMR.

References and notes

1 T. Nakamura, H. Fujii, N. Juni and N. Tsutsumi, *Opt. Rev.*, 2006, **13**, 104.
2 D. W. Mosley, K. Auld, D. Conner, J. Gregory, X. Q. Liu, A. Pedicini, D. Thorsen, M. Wills, G. Khanarian and E. S. Simon, *Proc. SPIE*, 2008, **6910**, 691017.
3 K. C. Krogman, T. Druffel and M. K. Sunkara, *Nanotechnology*, 2005, **16**, S338.
4 R. D. Allen, G. M. Wallraff, D. C. Hofer and R. R. Kunz, *IBM J. Res. Dev.*, 1997, **41**, 95.
5 (*a*) J. G. Liu and M. Ueda, *J. Mater. Chem.*, 2009, **19**, 8907; (*b*) Y. Suzuki, T. Higashihara, S. Ando and M. Ueda, *Macromolecules*, 2012, **45**, 3402.
6 C. A. Terraza, J. G. Liu, Y. Nakamura, Y. Shibasaki, S. Ando and M. Ueda, *J. Polym. Sci., Part A: Polym. Chem.*, 2008, **46**, 1510.
7 (*a*) N. H. You, Y. Suzuki, D. Yorifuji, S. Ando and M. Ueda, *Macromolecules*, 2008, **41**, 6361; (*b*) J. G. Liu, Y. Nakamura,

Y. Shibasaki, S. Ando and M. Ueda, *Macromolecules*, 2007, **40**, 4614; (*c*) J. G. Liu, Y. Nakamura, Y. Suzuki, Y. Shibasaki, S. Ando and M. Ueda, *Macromolecules*, 2007, **40**, 7902; (*d*) N. H. You, T. Higashihara, S. Yasuo, S. Ando and M. Ueda, *Polym. Chem.*, 2010, **1**, 480; (*e*) N. H. You, T. Higashihara, S. Ando and M. Ueda, *J. Polym. Sci., Part A: Polym. Chem.*, 2010, **48**, 656; (*f*) N. Fukuzaki, T. Higashihara, S. Ando and M. Ueda, *Macromolecules*, 2010, **43**, 1836.

8 N. Kakayama and T. Hayashi, *Prog. Org. Coat.*, 2008, **62**, 274.

9 C. Berti, A. Celli, E. Marianucci and M. Vannini, *Eur. Polym. J.*, 2006, **42**, 2562.

10 C. Berti, A. Celli, P. Marchese, E. Marianucci, C. Marega, V. Causin and A. Marigo, *Polymer*, 2007, **48**, 174.

11 H. J. Yen and G. S. Liou, *J. Mater. Chem.*, 2010, **20**, 4080.

12 (*a*) L. L. Beecroft and C. K. Ober, *Chem. Mater.*, 1997, **9**, 1302; (*b*) C. Sanchez, B. Lebeau, F. Chaput and J. P. Boilot, *Adv. Mater.*, 2003, **15**, 1969; (*c*) R. M. Laine, *J. Mater. Chem.*, 2005, **15**, 3725; (*d*) A. Zelcer, B. Donnio, C. Bourgogne, F. D. Cukiernik and D. Guillon, *Chem. Mater.*, 2007, **19**, 1992; (*e*) Z. Zhou, A. W. Franz, M. Hartmann, A. Seifert, T. J. J. Muller and W. R. Thiel, *Chem. Mater.*, 2008, **20**, 4986; (*f*) F. Pereira, K. Valle, P. Belleville, A. Morin, S. Lambert and C. Sanchez, *Chem. Mater.*, 2008, **20**, 1710; (*g*) Y. Y. Lin, C. W. Chen, T. H. Chu, W. F. Su, C. C. Lin, C. H. Ku, J. J. Wu and C. H. Chen, *J. Mater. Chem.*, 2007, **17**, 4571; (*h*) J. S. Kim, S. C. Yang and B. S. Bae, *Chem. Mater.*, 2010, **22**, 3549; (*i*) P. Xue, J. Wang, Y. Bao, Q. Li and C. Wuac, *New J. Chem.*, 2012, **36**, 903; (*j*) S. C. Yang, S. Y. Kwak, J. H. Jin, J. S. Kim, Y. Choi, K. W. Paikb and B. S. Bae, *J. Mater. Chem.*, 2012, **22**, 8874.

13 P. Gómez-Romero, and C. Sanchez, Hybrid Materials, Functional Applications. An Introduction, in *Functional Hybrid Materials*, ed. P. Gómez-Romero and C. Sanchez, Wiley-VCH Verlag GmbH & Co. KGaA, Weinheim, FRG, 2005, 1–14.

14 G. Kickelbick, Introduction to Hybrid Materials, in *Hybrid Materials: Synthesis, Characterization, and Applications*, ed. G. Kickelbick, Wiley-VCH Verlag GmbH & Co. KGaA, Weinheim, Germany, 2007, 1–48.

15 G. S. Liou, P. H. Lin, H. J. Yen, Y. Y. Yu, T. W. Tsai and W. C. Chen, *J. Mater. Chem.*, 2010, **20**, 531.

16 Y. W. Wang and W. C. Chen, *Compos. Sci. Technol.*, 2010, **70**, 769.

17 F. P. Glatz and R. Mulhaup, *High Perform. Polym.*, 1993, **5**, 213.

18 B. S. Rao, R. Sireesha and A. R. Pasala, *Polym. Int.*, 2005, **54**, 1103.

19 J. Crivello, *J. Polym. Sci., Polym. Chem. Ed.*, 1976, **14**, 159.

20 H. W. Su and W. C. Chen, *J. Mater. Chem.*, 2008, **18**, 1139.

21 (*a*) A. H. Yuwono, J. Xue, J. Wang, H. I. Elim, W. Ji, Y. Li and T. J. White, *J. Mater. Chem.*, 2003, **13**, 1475; (*b*) A. H. Yuwono, B. Liu, J. Xue, J. Wang, H. I. Elim, W. Ji, Y. Li and T. J. White, *J. Mater. Chem.*, 2004, **14**, 2978.

22 (*a*) D. Eder and A. H. Windle, *J. Mater. Chem.*, 2008, **18**, 2036; (*b*) M. Miyauchi, *J. Mater. Chem.*, 2008, **18**, 1858; (*c*) A. Yu, G. Q. Lu, J. Drennan and I. R. Gentle, *Adv. Funct. Mater.*, 2007, **17**, 2600; (*d*) D. Fattakhova-Rohlfing, M. Wark, T. Brezesinski, B. M. Smarsly and J. Rathousky, *Adv. Funct. Mater.*, 2007, **17**, 123.

23 P. Tao, Y. Li, A. Rungta, A. Viswanath, J. Gao, B. C. Benicewicz, R. W. Siegel and L. S. Schadler, *J. Mater. Chem.*, 2011, **21**, 18623.

